JOURNAL OF MATERIALS SCIENCE 33 (1998) 5473–5484

Toughening of epoxies through thermoplastic crack bridging

B. J. CARDWELL, A. F. YEE
Department of Materials Science and Engineering, University of Michigan, Ann Arbor, MI 48109, USA
E-mail: afyee@engin.umich.edu

The fracture toughness and toughening mechanism of two epoxy matrices containing varying concentrations of pre-formed polyamide-12 particles was investigated. The pre-formed thermoplastic modifier was used to keep the physical and morphological characteristics of the second phase constant while varying the matrix intrinsic toughness to simplify the interpretation of toughening results. We observed that these particles toughened the epoxies through a crack bridging mechanism involving large plastic deformation of the second phase. This mechanism was found to be effective independent of the potential of the matrix for plastic deformation since the increasing fracture toughness was accomplished without significant amounts of plastic deformation in the epoxy matrix. A quantitative model was adapted to account for the increase in toughness due to the crack bridging mechanism. From this model, it was possible to determine the factors which are most important when attempting to toughen a material through thermoplastic crack bridging. A better understanding of the specific factors which influence the efficiency of the crack bridging mechanism enables the fracture properties of brittle materials to be further improved with thermoplastic addition. This was shown to be very important when attempting to enhance the toughness of materials which are believed to be "un-toughenable" by conventional rubber modification, or materials whose other mechanical properties suffer from the addition of elastomeric materials.

1. Introduction

Thermosets are used extensively as adhesives, encapsulants, and as the matrix material in composites ranging from those used in aerospace structures to others in dental fillings. One pervasive problem with thermosets in such applications is their low fracture toughness. Consequently, a great deal of effort has been and is being expended to modify thermosets to increase their fracture resistance. The research reported here was motivated by a desire to toughen thermosets in dental applications. Such materials are usually extremely brittle and experience with attempts to toughen them suggests that the use of rubber is unlikely to be efficacious. The nature of the increase in fracture toughness by the addition of rubber particles has been discussed elsewhere in greater detail [1–6] and will not be covered here. When rubber additions are able to efficiently toughen a thermoset, it has been shown that the process usually involves enhanced localized shear yielding of the matrix. It has also been observed that as the cross-link density becomes greater, the effectiveness of rubber additions diminishes [4, 7–12]. This has been attributed to the decreasing ability of the thermoset to shear yield. Rubber addition reduces the modulus and creep resistance of the thermoset. This change is undesirable in many circumstances.

The use of modifiers which have high modulus and stiffness, such as inorganic fillers or glass, can limit the degradation of the mechanical properties of a thermoset. Unfortunately, the increases in toughness obtained by incorporating these types of materials has been shown to be only moderately effective [13–16]. An attractive compromise would be to use a rigid thermoplastic second phase to toughen a thermoset. Several researchers have had varying success using thermoplastics as a toughening agent [17–24]. Unfortunately, the important factors which influence toughening by the thermoplastic modifier are difficult to discern due to the method by which test specimens were prepared. The prevalent method in producing a thermoplastic second phase is to first dissolve the modifier into the epoxy resin and later precipitate it out during the curing process. This proves to be a very difficult process by which to create a series of materials with constant morphologies. There also exists the problems with phase inversion and the production of co-continuous networks with increasing amounts of thermoplastic modifier. These variables interfere with our ability to understand the results of systematically varying toughener type, concentration, and adhesion.

To eliminate the problems associated with precipitation of the thermoplastic phase, we designed a model

system using pre-formed thermoplastic particles to keep the morphology constant over various concentrations of second phase modifier. This also allows for much larger additions of the second phase to be made without causing a phase inversion. Additionally, the viscosity of the resin does not increase to the same extent as it would if the thermoplastic toughener were dissolved in the resin. Ultimately, we wish to find a general approach to thermosets which have increased fracture toughness without some of the disadvantages of rubber modification.

2. Experimental

2.1. Materials

Two epoxy matrix materials were chosen for this study. The first was comprised of a piperidine cured diglycidyl ether of bisphenol A (DGEBA) epoxy. The second was a 4,4'-diamino-diphenyl-methane (DDM) cured DGEBA epoxy. The selection of curing agents was made based on the "toughenability" of the resulting material. The piperidine cure produces a relatively brittle epoxy which is capable of limited shear deformation when rubber toughened while the DDM cured material was known to be difficult to toughen by conventional rubber additions due to its lower tendency to shear yield. The epoxy resin used for all of the specimens was a Dow epoxy resin sold under the trade name DER®331, which is a derivative of a DGEBA. This resin has an average molecular weight of 376 g/mole. Typical properties of the cured epoxy matrices can be found in Table I.

The model toughener was comprised of polyamide-12. Polyamide-12 was selected as the toughener because of its good adhesion with epoxy and its availability in the form of uniform spheres. The polyamide-12 has a product designation of SP500® and is manufactured by Toray Industries, Inc. The modifier exists as 8.0 μm average diameter spherical particles. No special surface treatment was applied. The polyamide-12 modified specimens used in this study contained various concentrations of these modifying particles. The exact compositions and corresponding properties are indicated in Table II.

To prepare the modified specimens, the epoxy was first heated to 110 °C to lower the viscosity of the resin, making it easier to disperse the polyamide-12 particles. The pre-formed particles were then added slowly and blended in by hand. The mixture was next held under a vacuum and mechanically stirred for 10 minutes to disperse the particles and degas the resin. Mixtures to which the DDM curing agent was to be added were held in an oven at 120 °C for 1.75 hours. The curing agent was then added, and the mixture was stirred for another 5 minutes. The epoxy was then poured into a preheated PTFE-coated mold and cured at 120 °C for 16 hours. Unmodified specimens were also prepared in the same manner, but without the polyamide-12 particle addition. Test specimens were machined from the as cut, 6.35 mm thick plaques.

It should be noted that lower particle-matrix adhesion was seen in earlier preparations of the DDM cured epoxy blends. It was deduced that the particle-matrix adhesion was affected by the amount of time that the polyamide-12 particles were in contact with liquid epoxy resin. Initially, the particles were not allowed the same time in contact with the liquid epoxy resin due to the vastly different gel times that the two curing agents produced. The gel time for the piperidine cured epoxy was approximately 2 hours at 120 °C, while the DDM caused gelation in about 15 minutes. With time, more of the relatively low molecular weight epoxy resin could diffuse into the surface of the particle, increasing the adhesion between the particle and matrix. Due to the presence of residual amine groups in the polyamide-12, the possibility of chemical reactions between the epoxy resin and the polyamide particles also existed.

The model system using pre-formed modifier allows much higher concentrations of thermoplastic to be added to the epoxy matrix without changing the

TABLE I Typical density and glass transition temperature for the cured epoxy matrix materials

Epoxy	Curing agent	Density (g/cm^3)	T_g (°C)
DER331 (DGEBA)	Piperidine	1.167	89
DER331 (DGEBA)	DDM	1.156	164

TABLE II Formulations, compressive properties, and fracture toughness of the toughened epoxy/polyamide-12 blends

Material description	Modifier PA-12 (*p.h.r.)	Curing agent Piperidine (*p.h.r.)	Curing agent DDM (*p.h.r.)	Volume fraction modifier	Modulus (GPa)	Yield stress (MPa)	K_{IC} (MPa m$^{0.5}$)
PIP	0	5	—	0.000	2.8	97	0.85
PIP/11	11	5	—	0.106	2.7	92	1.31
PIP/22	22	5	—	0.191	2.7	90	1.57
PIP/33	33	5	—	0.262	2.6	86	1.92
PIP/44	44	5	—	0.321	2.6	84	1.97
PIP/55	55	5	—	0.372	2.6	83	1.99
DDM	0	—	28	0.000	2.6	127	0.85
DDM/33	33	—	28	0.224	2.5	102	1.36
DDM/55	55	—	28	0.325	2.5	94	1.73
DDM/66	66	—	28	0.366	2.4	92	1.86

*p.h.r. = parts per hundred resin by weight.

mechanical properties and morphology of the second phase. In this way, the effect of particle properties such as: size, shape, volume fraction, mechanical behavior, and adhesion can be studied in greater detail in an attempt to determine the factors which are most important in trying to increase toughness using thermoplastic modifiers.

2.2. Fracture toughness measurements

All fracture toughness measurements were conducted using a pre-cracked specimen in a three point bending configuration. Three point bend single edge notch (3PB-SEN) specimens were machined to a length of 63.5 mm, a height of 12.7 mm, and a thickness of 6.35 mm. A small 1.5 mm deep notch was first cut into the center of the specimen using a jeweler's saw. A fresh razor blade, which has been chilled in liquid nitrogen, was then tapped into the cut with a hammer to create a pre-crack in the specimens. The specimens tested contained overall crack lengths which were a minimum of 4.0 mm and a maximum of 7.0 mm. These specimens were then loaded in a three point bend configuration using a servo-hydraulic Instron testing machine at a cross-head rate of 2.54 mm/s. The span of the three point bend apparatus was 50.8 mm.

Calculations using the stress intensity approach were used to quantify the fracture toughness of the test materials. Assuming linear elastic fracture mechanics apply at small displacements, the outer fiber stress, $\sigma_{\max}$, at the crack tip can be calculated as:

$$\sigma_{\max} = \frac{3S}{2BW^2} F_{\max} \tag{1}$$

where $F_{\max}$ is the maximum value of force required for fracture (N), B is the specimen thickness (m), W is the specimen width (m), and S is the span (m).

The critical value of the stress intensity factor, K_{IC}, can be calculated using the equation:

$$K_{\mathrm{IC}} = Y\sigma_{\max}(a)^{0.5} \tag{2}$$

For the specimen geometry used, the geometry factor, Y, can be determined by the equation [25]:

$$Y = 1.93 - 3.07(a/W) + 14.53(a/W)^2 - 25.11(a/W)^3 + 25.80(a/W)^4 \tag{3}$$

where a is the crack length (m).

2.3. Study of the process zone

The effects of the thermoplastic second phase in various concentrations were examined at the crack tip in specimens which were both critically and sub-critically loaded. Sub-critically loaded cracks were obtained by using a double side notch specimen in four-point-bending, 4PB-DSN. This method is described in detail by Sue *et al*. [26]. Ideally, this method simultaneously produces a crack which has failed and another which has been sub-critically loaded which retains accumulated damage at a point just before failure. To produce such a sub-critically loaded crack, two nearly identical cracks are made on the same edge of a specimen. The specimen is then loaded in the four-point bend configuration until one of the cracks has failed. The failure of one crack unloads the other crack which has undergone some growth or has accumulated some damage. The sub-critically loaded crack tip can now reveal the structure of the process zone preceding failure using various microscopy techniques. Thin sections were made at the midplane and the process zone could be observed using transmitted light microscopy.

Petrographic thin sections obtained from the 4PB-DSN method were observed at various magnifications in transmitted light mode using a Nikon Optiphot microscope. The thickness of these thin sections ranged from 0.13 to 0.50 mm. Although the thickness was varied for clarity, the thickness of the specimens for any microscopy which are presented for comparison were kept constant.

Fracture surfaces were observed using scanning electron microscopy (SEM) techniques. These postmortem microscopy specimens were obtained from the remnants of three point bend fracture specimens. Photographs were taken from the center of the fracture surface in the planestrain region. Electron microscopy specimens were first sputtered very lightly with gold-palladium to reduce charging and were then observed in a Hitachi S-800 scanning electron microscope at 2 kV accelerating voltage at a 5.0 mm working distance.

3. Results

Fracture toughness, modulus, and compressive yield strength are shown in Table II. It can be seen that the presence of the thermoplastic phase can significantly increase the fracture toughness of both of the epoxy matrix materials with only relatively small decreases in the compressive modulus and yield strength.

Fig. 1 shows the optical micrograph obtained from the 4PB-DSN experiment of a 33 parts per hundred resin by weight (p.h.r.) polyamide-12 piperidine cured blend which is representative of the other blends. It can be seen that the crack tip exhibits no significant birefringence when viewed through crossed polarizers. This would indicate the absence of significant plastic shear deformation of the matrix before failure.

Fig. 2 contains the critically loaded crack viewed between crossed polarizers. The only birefringence arises from the yielded particles of polyamide-12 on the fracture surface. It can also be seen in these photographs that very little sub-surface damage formed during fracture. Particles away from the fracture surface did not plastically deform, else they would have produced plastic birefringence.

Closer examination of the fracture surface itself using a SEM (Fig. 3) shows the presence of highly drawn particles of polyamide-12 in the process zone ahead of the pre-crack. It can be seen that the particles adhere well to the matrix and are capable of large plastic strains before failure. It is also apparent from the large

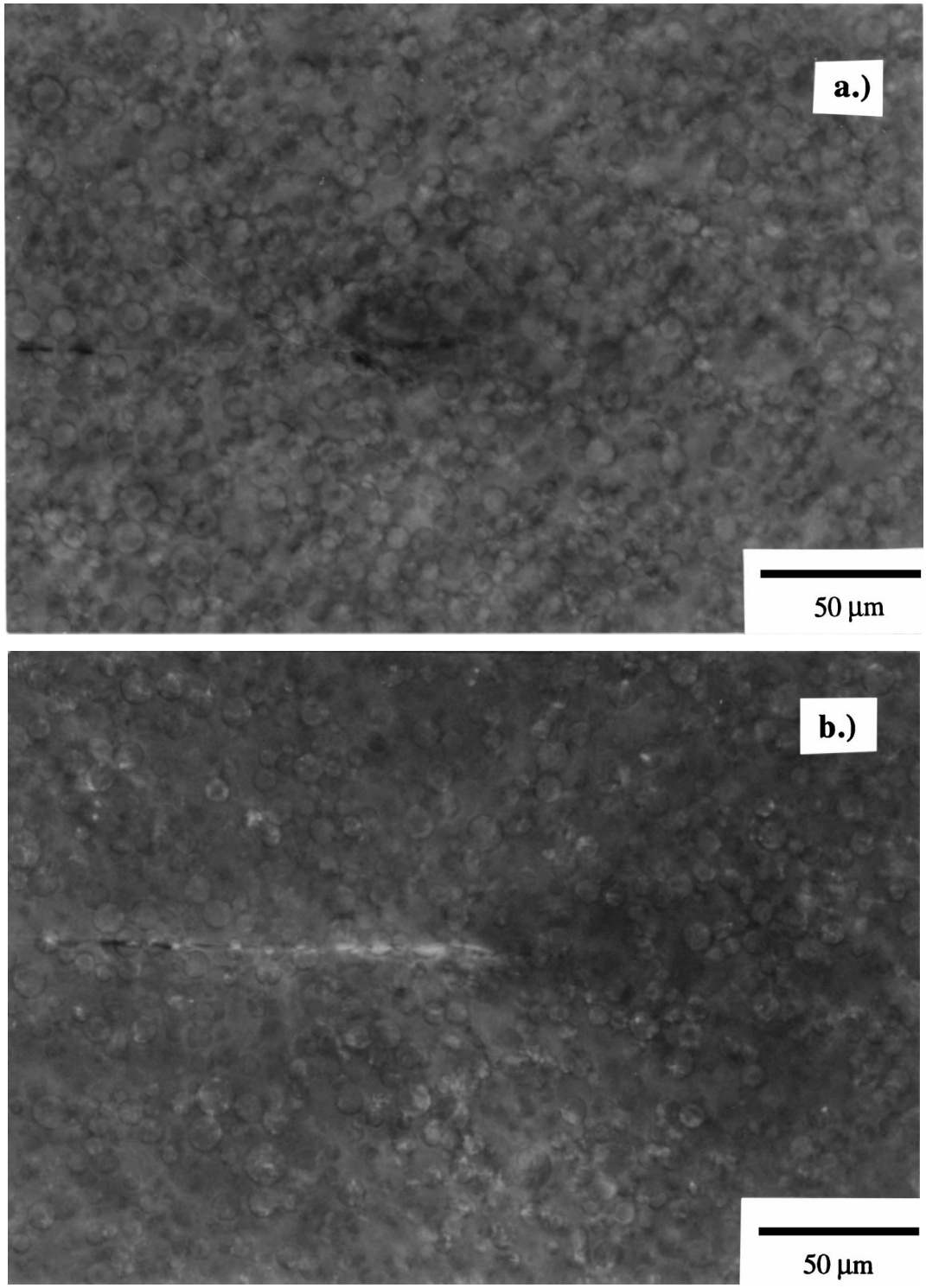

Figure 1 Optical micrographs of the sub-critically loaded crack obtained from a 4PB-DSN specimen (a) transmitted light and (b) transmitted light with crossed polarizing filters.

deformations that the particles failed well after the crack had advanced through the matrix. Fig. 4 shows the presence of intact particles "bridging" a crack which has advanced in a sub-critically loaded 11 p.h.r. polyamide-12 piperidine specimen.

The three-point-bending geometry is inherently unstable to continued crack growth. In the unstable fracture region of the fracture surface (Fig. 5) it can be seen that the particles show no extension and were simply cleaved due to the velocity of the advancing crack. The same behavior is seen for all of the compositions tested. The main difference is the number of second phase particles which the crack intersects due to concentration of the polyamide-12.

The absence of obvious plastic deformation in the epoxy matrix in conjunction with limited sub-surface cracking and damage indicate the bulk of the toughening is due to the presence and plastic deformation of the thermoplastic second phase. We conclude that this material system is toughened by a crack bridging mechanism similar to ones which were originally proposed for rubber toughening [27, 28]. It was estimated

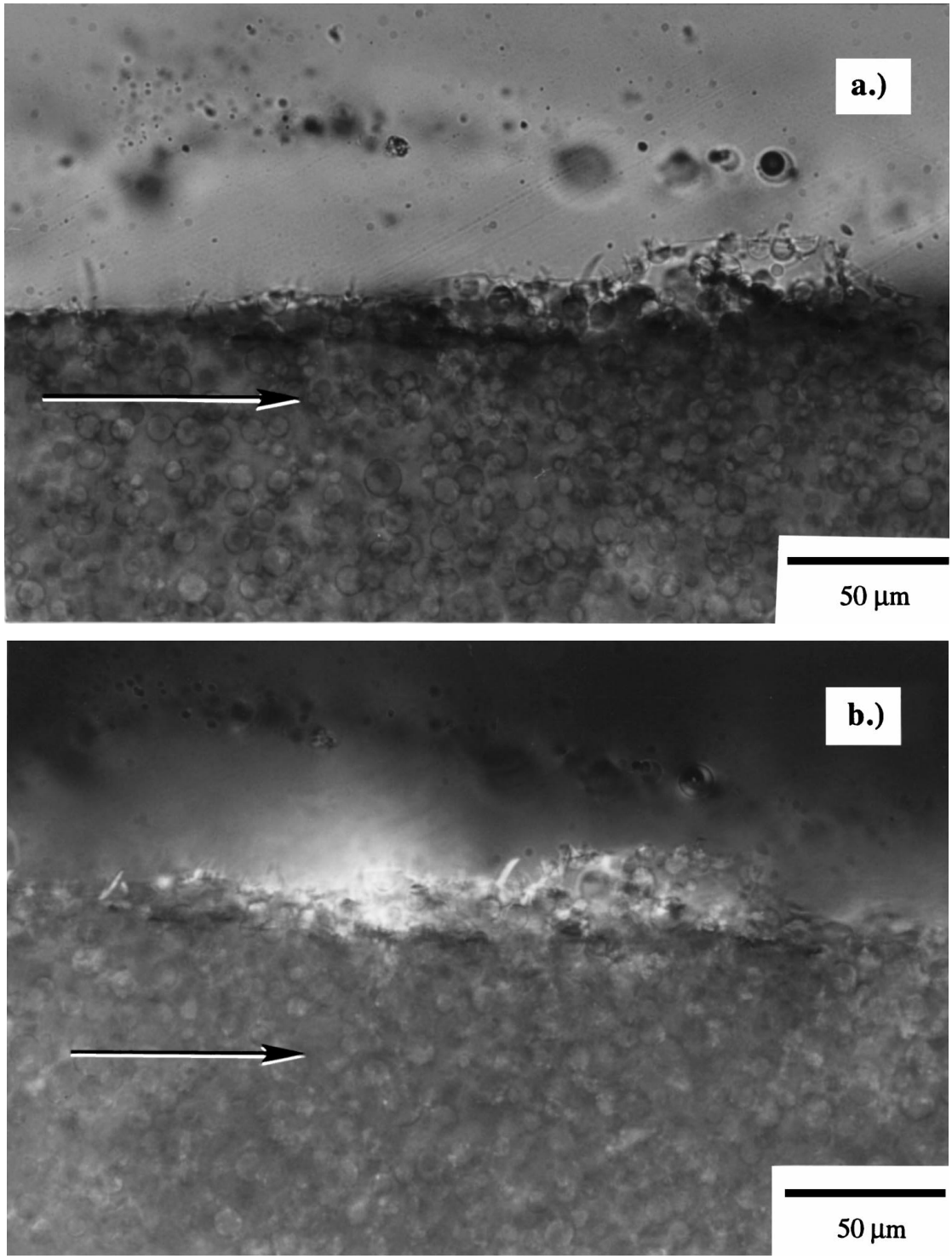

Figure 2 Optical micrographs of the critically loaded crack obtained from a 4PB-DSN specimen (arrow indicates direction of crack propagation). (a) Transmitted light and (b) transmitted light with crossed polarizing filters.

that stretching and tearing of rubber particles during crack bridging in rubber modified epoxies could only account for a small amount of the measured toughness due to the relatively poor mechanical properties of rubber [29]. Crack bridging by ductile thermoplastic particles should be a much more effective mechanism. Toughening could occur in two ways. First, the presence of the thermoplastic particles reduces the stress intensity seen at a crack tip by applying a crack closing traction. Second, as the crack opening displacement increases, the particles cold draw. Plastic deformation and strain hardening of the second phase thermoplastic are also thought to make this process more efficient at toughening the material because it transfers the stress concentrated at the crack tip to a larger region, thus allowing more of the second phase material to become involved in the deformation processes. Had we used a specimen geometry that allows stable crack growth we would probably have witnessed an R-curve behavior (i.e. where the crack growth resistance increases with crack propagation until a steady-state resistance is reached).

Figure 3 SEM micrograph showing the deformed polyamide-12 particles on the fracture surface a polyamide-12 modified epoxy from within the process zone (arrow indicates direction of crack propagation).

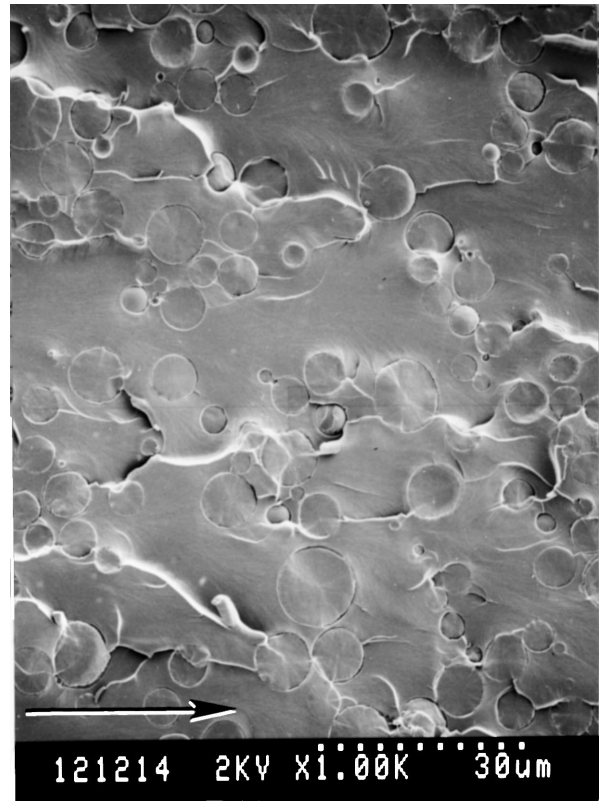

Figure 5 SEM micrograph showing the fast fracture region of the fracture surface (arrow indicates direction of crack propagation).

4. Discussion

Other researchers have also investigated the effectiveness of thermoplastic additions to an epoxy matrix and have reported varying results. Bucknall and Partridge [17] investigated the effects of dissolving poly (ether sulphone) into epoxy resins and obtaining phase separated structures. Their investigation generated various one- and two-phase materials depending on the type of resin used and the amount of modifier added. It was found that the additions of poly(ether sulphone) had very little effect on the fracture toughness of the epoxy, but these additions also did not lower the modulus of the blends. Later work by Bucknall and Gilbert [18]

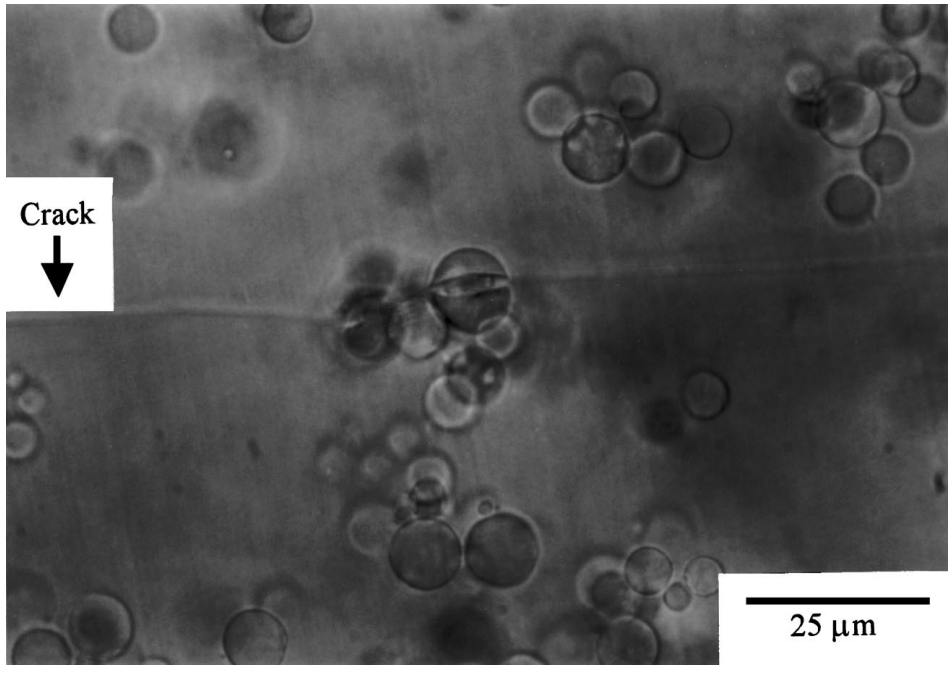

Figure 4 Optical micrographs of a bridging particle in a sub-critically loaded crack (arrow indicates direction of crack propagation).

show that the additions of poly(ether imide) to a high T_g epoxy exhibits an improvement in fracture toughness which is attributed to a drawing mechanism in the additive. Due to a changing morphology, it is difficult to distinguish the important factors which affect the resulting toughness in these materials.

Kim and Brown [19] have also attributed an increase in toughness in an epoxy modified with a glassy thermoplastic second component to the deformation of the latter, but the toughness significantly increased only after phase inversion occurred, making the modifier the continuous matrix. The observation of an increase in toughness accompanying phase inversion was also made by both MacKinnon *et al.* [20] and Hourston and Lane [21] on different material systems. Additionally, it was noted that as the modifier phase becomes the continuous matrix, the mechanical properties of the material decrease more significantly. It can also be assumed that other properties, such as chemical resistance, also suffer as the cross-linked fraction of the system becomes the dispersed phase.

Hedrick *et al*. [22, 23] were able to moderately increase the fracture toughness of an epoxy matrix without significantly reducing its flexural modulus. In these investigations, several molecular weights of poly(arylene ether sulphone)s were used in various concentrations. The increase in toughness was attributed to the ductile nature of the polysulphone-rich phase and possible crack pinning due to the particles. It was also found that as the molecular weight of the polysulphone surpassed a critical level for ductile behavior, the fracture toughness of the materials also increased to a larger extent. Unfortunately, as molecular weight increased, there was an accompanying change in the size of the second phase particles making only a qualitative interpretation of these results possible. Results obtained by Kim and Robertson [24] also show that a material can be toughened through the use of a crystalline thermoplastic second phase with very little decrease in modulus. These authors suggested that the toughening could be due to phase transformation of the crystalline phase. The current results suggest that the toughening effect they observed could also be explained by the mechanism proposed here.

The results recited above demonstrate that thermoplastic modifiers can be used to increase the toughness of an epoxy matrix. This can be achieved in some circumstances without degrading the mechanical properties of a thermoset. In this investigation, a modest lowering of the modulus accompanied the addition of thermoplastic particles. This is most likely due to the lower modulus of the polyamide-12 particles (roughly 2.0 GPa) than that of the epoxy. However there is no evidence in this, or any other investigation, to indicate that a thermoplastic modifier must have a substantially lower modulus to toughen by the observed mechanisms. The modulus of the modified epoxy could be left unaffected by selecting a modifier with a modulus comparable to or even higher than that of the epoxy matrix. This would be extremely difficult to achieve using rubber additions.

4.1. Quantitative bridging model

Various researchers [32–42] have offered quantitative descriptions of the toughening effect of unbroken ligaments stretching in the wake of an opening crack in brittle ceramic or metallic materials. All of these solutions have the same physical basis and differ mainly in the assumptions made regarding crack opening displacement, deformation behavior of the ductile phase, and the stress distribution found in the bridging zone. Numerical solutions have also been presented in terms of both stress intensity (K) and strain energy release rate (G). Evans and McMeeking [33] have shown that analysis of crack bridging can be conducted equally by either method. It was desired to adapt one such model to quantitatively describe the behavior of crack bridging in the model polyamide-12 modified epoxy blends. It was also desired to verify or reduce the number of assumptions made in such a numerical solution.

Work on brittle ceramics toughened by a ductile metallic second phase was performed by Przystupa and Courtney [32], from which a general quantitative model of toughening due to the plastic deformation of a ductile phase was obtained. This model assumed that the increase in the toughness was due to the spanning, or bridging, of the crack faces by the plastically deforming second phase. They also proposed that there may be a contribution to crack front bowing between the impenetrable particles. Their model took a stress intensity approach in determining the quantitative toughening effect due to the second phase. This stress intensity approach lent itself very well to the type of toughness data which was obtained for the thermoplastic modified epoxy blends.

They calculated the apparent fracture toughness, K_C, of a brittle material containing ductile inclusions as:

$$K_C = K_{EX} \geq AK_{CRM} + K_p \tag{4}$$

where K_{EX} is the stress intensity of external forces, K_{CRM} is the critical stress intensity of the matrix, K_p is the stress intensity of unbroken particles, and A accounts for crack bowing.

K_p acts as a crack closing force for which the stress intensity is calculated as [43]:

$$K_p = \sqrt{\frac{2}{\pi}} \int_0^{X_{PZ}} \frac{\sigma_P}{\sqrt{X}}\, dX \tag{5}$$

where σ_P is the stress in the process zone, and X_{PZ} is the size of the process zone.

They assumed that the properties of the ductile particle obey a constitutive relation of the Ramberg-Osgood form:

$$\sigma = C\varepsilon^n \tag{6}$$

and

$$\sigma_P = fC\varepsilon^n \tag{7}$$

where f is the inclusion volume fraction, C is the power-law hardening coefficient, and n is the power-law hardening exponent.

To simplify the calculations, the length of the deformed region of the inclusions was taken as constant. Hence, the maximum principal particle strain was taken as

$$\varepsilon = \frac{V}{h} \tag{8}$$

where h is the particle "gauge length" subjected to plastic strain between fractured surfaces for a given volume fraction, and V is the crack opening displacement normal to the crack surface at any given point away from the crack tip for a crack [43]:

$$V = \frac{8AK_{\mathrm{CRM}}}{E'_{\mathrm{m}}\sqrt{2\pi}}\sqrt{X} \tag{9}$$

where E'_{m} is the matrix modulus, E_{m}, for plane stress conditions (or which equals $E_{\mathrm{m}}/(1-\nu^2)$ for plane strain conditions where ν is Poisson's ratio) and X is the distance from the crack tip.

If the critical strain to failure for the plastic particles ($\varepsilon_{\mathrm{CR}}$) is known, Equations 8 and 9 can be combined and rearranged to calculate the process zone size (X_{PZ}) as:

$$X_{\mathrm{PZ}} = 2\pi\left\{\frac{hE'_{\mathrm{m}}\varepsilon_{\mathrm{CR}}}{8AK_{\mathrm{CRM}}}\right\}^2 \tag{10}$$

Combining the above equations gives:

$$K_{\mathrm{C}} \geq AK_{\mathrm{CRM}} + \frac{fCE'_{\mathrm{m}}\varepsilon_{\mathrm{CR}}^{n+1}}{2(n+1)AK_{\mathrm{CRM}}}h \tag{11}$$

It was noted that $(C\varepsilon_{\mathrm{CR}}^{n+1}/(n+1))$ is a measure of the particle plastic work to failure, G_{p}, obtained from integrating Equation 6; so that K_{C} could be written as:

$$K_{\mathrm{C}} \geq AK_{\mathrm{CRM}} + \frac{E'_{\mathrm{m}}fG_{\mathrm{p}}h}{2AK_{\mathrm{CRM}}} \tag{12}$$

Unfortunately, since the values for A and h cannot be calculated *a priori*, the predictive power of such a model is limited. These terms must be further arranged to enable one to use this model to predict the toughness which can be obtained by crack bridging. Several assumptions have been made in the derivation of Equation 12 which are in need of further investigation in our material system.

4.2. Crack opening displacement

In modeling the bridging process, it was assumed in Equation 9 that the crack opening displacement could be estimated using linear elastic fracture mechanics (LEFM). This crack opening displacement was calculated based on the shape which a crack would attain in an elastic medium of a known critical stress intensity. The crack shape assumed for this model was that of the unmodified matrix material, which does not take into account the increase in toughness due to crack closing tension from the bridging particles and their effect on the crack opening displacement. This assumption was made to reduce the immense problems associated with obtaining exact numerical solutions for the crack opening displacement.

Bannister *et al.* [40] added lead particles to a glass matrix to investigate the role of the ductile metal phase in crack bridging. In this study, the crack opening displacement was measured microscopically on a loaded crack which contained bridging lead particles. Their results demonstrated that the crack opening displacement follows the elastic solution at small distances behind the crack tip (<2.5 mm). This suggests that the elastic solution is a good approximation in cases where the length of the bridged zone is relatively small. It is likely that the approximation is valid for purposes of this investigation, since the bridged zone was found to be less than 250 μm. It should be noted that if the size of the process zone increases in more efficient bridging systems, the elastic approximation for crack opening displacement may no longer be valid, and may require a more exact solution for crack opening displacement.

4.3. Constraint of the ductile phase

Przystupa and Courtney assumed that the deformation behavior of the ductile bridging particles followed an approximate exponential strain hardening relationship in determining the stress within the bridging zone in Equation 7. This relationship for mechanical behavior is obtained from unconstrained specimens tested in uniaxial tension. Work on lead wires embedded in glass by Ashby *et al.* [36] has shown that the deformation behavior of metal differs when placed under constraint. In this investigation, several qualitative degrees of adhesion were observed at the lead-glass interface producing different amounts of constraint. Debonding was seen to decrease the amount of constraint and produce changes in a normalized load-displacement plot. Higher constraint was seen to increase the peak stress while lowering the amount of energy which was absorbed during deformation. Debonding tended to lower the peak stress which was seen in the wire, but the amount of energy which was absorbed during plastic deformation increased. It was also found that changing the initial diameter of the wire from 1.3 mm to 2.1 mm did not change the normalized values for peak stress and energy. These results were later supported by Bannister and Ashby [39] on thin sheets of lead constrained between panes of glass in which the amount of debonding could be better controlled, and by Cao *et al.* [37] on constrained wires. These experiments demonstrated the importance of debonding and constraint on the efficiency of a ductile bridging phase to toughen, since the present bridging model relies heavily on the ductile work to failure of the second phase. Lower constraint caused by limited debonding increases the total energy absorbed during the deformation process while increasing the ultimate elongation of the second phase material.

4.4. Bridging potential

The experimental methods introduced by Ashby *et al.* [36, 39] allowed us to greatly enhance the predictive power of the Przystupa and Courtney model. Since a value for the effective gauge section (h) could not be predicted *a priori* and the plastic work to failure (G_p) could be influenced by constraint, it was desired to replace these terms with a single variable which could be more accurately determined experimentally. When a crack opening displacement (V) increases from zero, the particle elongates. This change in elongation (Δh) for a gauge section of constant longitudinal strain (ε) and uniform initial area is equal to V. The strain in this section is found to be:

$$\varepsilon = \frac{\Delta h}{h} = \frac{V}{h} \tag{13}$$

Rearranging, the crack opening displacement is found to be:

$$V = h\varepsilon \tag{14}$$

Since G_p is the area under the stress-stain curve of the ductile second phase, it can be shown that the bridging potential (W_P) of the embedded ductile phase of a given gauge length is:

$$W_P = \int_0^{V_{CR}} \sigma(V)\,dV = h\int_0^{\varepsilon_{CR}} \sigma(\varepsilon)\,d\varepsilon = hG_p \tag{15}$$

The bridging potential can therefore be determined from the area beneath the nominal stress-strain curve when it is plotted as a function of crack opening displacement and has the units of J/m^2.

It was possible to experimentally obtain values for W_P for different matrix materials, ductile inclusions, and interfacial adhesion using a test geometry similar to the one introduced by Bannister and Ashby [39] with minor modifications. This method allows the mechanical behavior of a material to be experimentally determined while under constraint, which approximates the deformation of a bridging particles. This is possible when it is assumed that the normalized values obtained from such macroscopic experimental specimens can be used to describe the behavior of the much smaller bridging particles. This was believed to be a valid assumption because Ashby demonstrated that the stress-displacement results obtained for both constrained sheets and constrained wires were alike once normalized. This indicated that the values obtained for displacement scaled with initial thickness or diameter of the constrained material.

Fig. 6 illustrates the specimen configuration for the testing of a thermoplastic sheet in constraint. A thin sheet consisting of polyamide-12 was produced to model the behavior of the thermoplastic particles added to the epoxy resins. This 230 μm sheet was compression molded to reduce the effects of orientation and then bonded to thick sections of the identical DGEBA epoxy cured with piperidine used earlier to approximate the adhesion between the polyamide-12 and the matrix found in the original particulate-modified blends. These cured specimens contained PTFE release film which acted as pre-cracks in the specimens. These specimens were then tested in uni-axial tension to obtain the behavior of nominal stress with displacement.

The values obtained for stress were normalized with respect to the yield stress of unconstrained polyamide-12 sheets ($\sigma_0 = 43.5$ MPa) and the displacements were normalized with respect to the initial sheet thickness (t). To determine the appropriate area beneath this normalized curve, certain boundaries must be drawn. An initial peak in the load-displacement behavior was observed. A drop from this initial peak was accompanied by an audible sound, probably due to rapid crack growth which indicated that this load drop was due to the failure of a small ligament of epoxy present in the pre-crack. The area contained within this initial peak was therefore not considered in the determination of the bridging potential of the polyamide-12. In any case, the amount of area within this peak was small compared to the total area under the load-displacement curve.

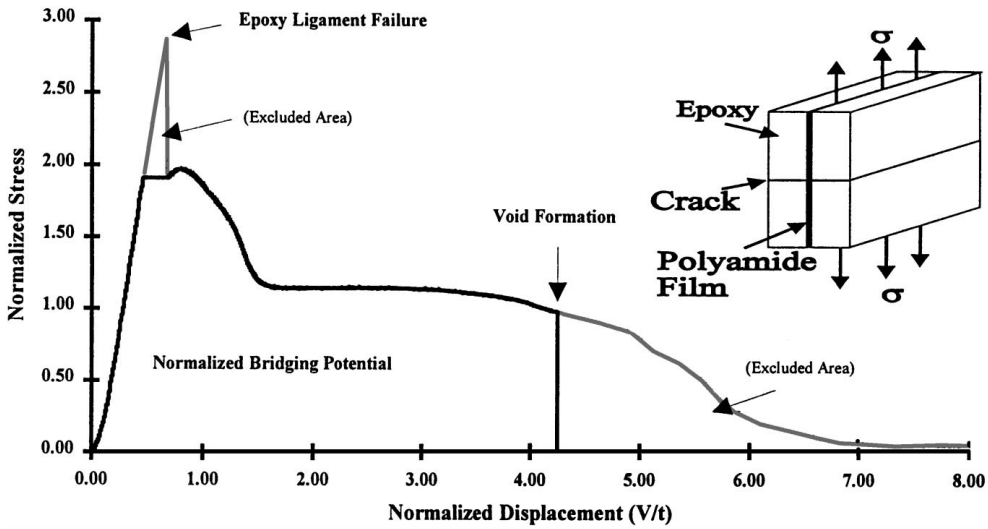

Figure 6 An example of a normalized stress (σ/σ_0)-normalized displacement (V/t) curve obtained from a polyamide-12 sheet in constraint showing area used to calculate bridging potential.

The polyamide-12 sheet was also observed to begin a voiding process during later stages of elongation due to the presence of slight variations in its thickness. The initiation of this voiding coincided with a drop in the load during deformation. This point more accurately describes the ultimate elongation of a constrained sheet because a reduction in lateral constraint of the thermoplastic from the formation of voids allows further elongation of remaining ligaments. It is likely that an ideally homogeneous thermoplastic sheet would reach its ultimate elongation and fail at the initiation of this voiding process. The elongation at this stage was also observed to be quite consistent with the plastic deformation measured in microscopic particles. The extension at which voiding of the polyamide-12 sheet began was therefore chosen as the upper bound of the deformation process when calculating the bridging potential.

An example plot of these normalized values is included in Fig. 6. Also indicated on this plot are the boundaries and area used in the bridging potential calculations. This bounded area represents a normalized bridging potential for this thermoplastic-matrix combination, and is equal to:

$$\text{Area} = \frac{W_P}{t\sigma_0} \tag{16}$$

where t is the initial sheet thickness and σ_0 is the yield stress of the unconstrained thermoplastic.

To extract the bridging potential for the spherical particles used in this investigation, the normalized area was multiplied by both the yield stress of unconstrained material (σ_0) and the 8.0 μm average particle diameter (d) of the polyamide-12. In doing this, it was assumed that the behavior of small spheres was similar to that of the semi-infinite sheet of polyamide-12 so that $d \approx t$.

4.5. Model results

Inserting Equation 15 into Equation 12 we obtain:

$$K_C \geq AK_{CRM} + \frac{E'_m f W_P}{2AK_{CRM}} \tag{17}$$

Values pertaining to the polyamide-12 modified epoxy blends were next inserted into this equation to explore its validity. Certain assumptions were necessary in order to obtain the parameters required by this quantitative model.

To determine the importance of the crack bowing parameter (A) the work of other researchers is considered. The effect of the pinning and subsequent bowing of a crack front due to the presence of inhomogeneities in a material was qualitatively described by Lange [44]. His analysis suggests that an increase in fracture toughness is possible due to pinning, but inhomogeneities may also reduce the strength of a material by introducing stress concentrations. Later work by Evans [45] confirms that crack bowing due to the interaction of an advancing crack front with impenetrable obstacles increases the fracture strength of a brittle material. Evans shows that the effect due to crack bowing increases with the volume fraction of the second phase due to a drop in the inter-particle spacing. Evans also points out that crack bowing makes only a minor contribution to the toughness in fiber reinforced composites where fiber pullout is present and in materials in which the second phase is ductile because a crack may more easily circumvent the inclusions. Work on epoxies containing glass spheres by Kinloch *et al.* [46] also shows a reduction in the effectiveness of this mechanism when debonding of the second phase occurs. Recent work in our laboratory on a similar system shows that the effect of crack bowing on toughness is negligible [47].

In the present work microscopic evidence for crack bowing can be seen in Fig. 3 and especially in Fig. 5 where the particles act more as impenetrable objects due to the high velocity of the advancing crack. The exact contribution from crack bowing is not known due to the deviations from ideality. It was therefore desired to obtain an upper bound for the crack bowing parameter. Since it is known that the effects due to crack bowing increase with the volume fraction of second phase material, this upper bound was assumed to occur at the maximum volume fraction of added polyamide-12 (approximately 35%). For randomly dispersed impenetrable obstacles, the crack bowing parameter (A) was estimated to be in the range of approximately 1.5 to 2.0 for this volume fraction [32, 45]. Since the second phase material used in this investigation was of a ductile nature and evidence existed of limited debonding, it was believed that the contribution to the overall toughness due to crack pinning and bowing was minor. A rapidly approaches 1.0 at low volume fractions due to an increase in interparticle spacing. Therefore, to reduce the number of fitting parameters present in this analysis, the average value of the crack bowing parameter (A) was assumed to be unity and independent of the volume fraction (f). Since K_{CRM} is $\ll K_C$ this simplification should introduce only a small error.

W_P was determined experimentally using polyamide-12 sheets under constraint as described earlier. Values for the critical stress intensity, matrix modulus, and volume fraction modifier were also obtained experimentally. To further insure validity of the model, it was also assumed that the behavior of the particles was identical in the two epoxy test systems and the only variable was the modulus of the matrix material. This eliminated many of the degrees of freedom which would be introduced by changing the particle parameters. Table III lists the values given to each variable in the model.

Fig. 7 is a plot of the data collected for both the epoxy systems and the corresponding plots of the theoretical

TABLE III Variables and their values used in quantitative bridging model calculations

Variable	Symbol	Value
Crack bowing constant	A	1
Critical stress intensity of matrices	K_{CRM}	0.85 MPa $m^{0.5}$
DER331/Piperidine matrix modulus	E_m	2.83 GPa
DER331/DDM matrix modulus	E_m	2.59 GPa
Bridging Potential of 8.0 μm Polyamide-12 Particles	W_P	1.73E-03 MPa m (MJ/m^2)

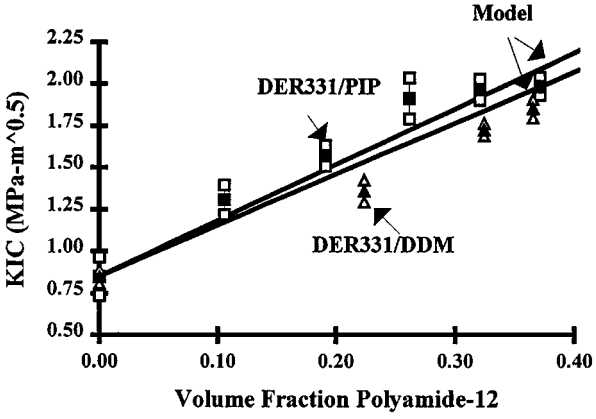

Figure 7 Plot showing the toughness of polyamide-12 modified epoxies with the theoretical curves obtained from the bridging model.

fracture toughness as predicted by the model described above. It can be seen that the toughening model actually fits the experimentally obtained fracture toughness data quite well due to the relative simplicity of fracture behavior in the two systems. The model also predicts the lower fracture toughness of the DDM cured epoxy blend due to its lower modulus. Some deviations from the model exist and are likely to be due to oversimplified assumptions made regarding the deformation behavior of the matrix and particles, differences in the particle-matrix interfacial adhesion in the two systems, deviations in the measured values, and changes in material behavior due to increased strain rates found at the crack tip. Differences in the morphology of the pre-formed particles and the compression molded sheet from which we obtained stress-strain properties could have resulted in further deviations. It should also be noted that this model is limited to the effect of particles bridging on one plane. Some crack deflection or bifurcation can be caused by thermoplastic inclusions which can increase the observed toughness.

Although all of the characteristics which define the most effective thermoplastic modifier have not yet been elucidated, this work and other previous investigations indicate that the most efficient thermoplastic toughening agents exhibit large work-to-fracture, i.e. they were able to plastically deform and draw by strain hardening. We also note that the materials which were significantly toughened by thermoplastics possessed good adhesion between the modifier and the matrix material [30, 47, 48]. Without this adhesion, the second phase could prematurely de-bond before deformation could occur. We can also hypothesize that if the adhesion were too high, the extent of plastic deformation which the thermoplastic undergoes would be limited due to excessive constraint of the second phase. This constraint would limit the amount of material which could be involved in a bridging and deformation process. However, it is still unclear what the optimal amount of adhesion or other thermoplastic modifier properties are necessary to optimize this method of toughening. Further study is needed to determine these factors before highly effective thermoplastic toughened epoxy systems can be efficiently produced. It is hoped that this method of using a pre-formed modifying particle as the toughening agent can help in better elucidating the factors which most influence the fracture behavior of thermoplastic modified epoxies. Finally, we note that Pearson [31] has shown that by adding a rubbery phase to thermoplastic particles, cavities can form inside the particles thereby producing an enhanced toughening effect. Whether or not bridging also contributes to the toughening mechanism in this system has yet to be investigated.

An interesting note may be made regarding the ability of the 3PB-SEN specimen testing geometry to produce the crack initiation toughness. Clearly the intrinsic toughness of the epoxies has not increased as a result of the addition of the polyamide particles. Thus, all increases in toughness observed occurred in the wake of the crack. This observation may have important implications regarding toughening results that have been reported in the literature using a similar specimen geometry. The toughening observed may also be due to wake effects. In fact this was reported to be the case in rubber modified epoxies [49].

5. Conclusions

The addition of a thermoplastic second phase can significantly increase the fracture toughness of epoxy blends. The toughening in this case is due to crack bridging and plastic deformation of the second phase and need not be accompanied by substantial shear deformation of the epoxy matrix material. The various factors which control the effectiveness of this toughening are easier to discern by adding a pre-formed modifier to better control morphology and mechanical properties of the second phase. It has been shown that material systems which were thought to be un-toughenable can benefit from thermoplastic modification. This is made possible because the mechanism by which the epoxy blend was modified in this investigation did not require plastic deformation of the matrix. This demonstrates that polymeric materials which are unable to significantly plastically deform could take advantage of this toughening method just like ceramic materials.

A quantitative model was successfully adapted to account for the increase in toughness due to the crack bridging mechanism. From this model, it was possible to determine the factors which are most important when attempting to toughen a material through thermoplastic crack bridging. A better understanding of the specific factors which influence the efficiency of the crack bridging mechanism enables the fracture properties of brittle materials to be further improved with thermoplastic additions.

Acknowledgements

This research was supported by grant number 032562 from the National Institute of Dental Research to the Specialized Materials Center in the School of Dentistry at the University of Michigan. The authors would also like to thank Michael Groleau for assistance in the preparation of the epoxy blends.

References

1. A. J. KINLOCH and R. J. YOUNG, "Fracture Behavior of Polymers" (App. Sci. Publishers, London, 1983).
2. A. F. YEE and R. A. PERASON, *J. Mater. Sci.* **21** (1986) 2462.
3. R. A. PERASON and A. F. YEE, *ibid.* **21** (1986) 2475.
4. A. F. YEE and R. A. PERASON, *ibid.* **24** (1986) 2571.
5. A. J. KINLOCH, S. J. SHAW, D. A. TOD and D. L. HUNSTON, *Polymer* **24** (1983) 1341.
6. A. J. KINLOCH and D. L. HUNSTON, *J. Mater. Sci. Lett.* **5** (1986) 909.
7. C. MEEKS, *Polymer* **15** (1974) 675.
8. J. N. SULTAN, R. C. LIABLE and F. J. McGARRY, *App. Polym. Symp.* **16** (1971) 127.
9. J. M. SCOTT, G. M. WELLS and D. C. PHILLIPS, *J. Mater. Sci.* **15** (1980) 1436.
10. W. B. CHERRY and K. W. THOMPSON, *ibid.* **16** (1981) 1913.
11. T. D. CHANG and J. O. BRITTAIN, *Polym. Eng. Sci.* **22** (1982) 1228.
12. T. K. CHEN and H. J. SHY, *Polymer* **33** (1992) 1656.
13. F. F. LANGE, *Phil. Mag.* **22** (1971) 983.
14. A. G. EVANS, *ibid.* **26** (1972) 1327.
15. A. G. EVANS, S. WILLIAMS and P. W. R. BEAUMONT, *J. Mater. Sci.* **20** (1985) 3668.
16. A. J. KINLOCH, D. L. MAXWELL and R. J. YOUNG, *ibid.* **20** (1985) 4169.
17. C. B. BUCKNALL and I. K. PARTRIDGE, *Polymer* **24** (1983) 639.
18. C. B. BUCKNALL and A. H. GILBERT, *ibid.* **30** (1989) 213.
19. S. C. KIM and H. R. BROWN, *J. Mater. Sci.* **22** (1987) 2589.
20. A. J. MacKINNON, S. D. JENKINS, P. T. McGRAIL and R. A. PETHRICK, *Macromolecules* **25** (1992) 3492.
21. D. J. HOURSTON and J. M. LANE, *Polymer* **33** (1992) 1379.
22. J. L. HENDRICK, I. YILGOR, G. L. WILKES and J. E. McGRATH, *Polym. Bull.* **13** (1985) 201.
23. J. L. HENDRICK, I. YILGOR, M. JUREK, J. C. HENDRICK, G. L. WILKES and J. E. McGRATH, *Polymer* **32** (1991) 2020.
24. J. K. KIM and R. E. ROBERTSON, *J. Mater. Sci.* **27** (1992) 161.
25. W. F. BROWN, J. E. SRAWLEY, *ASTM STP 410* (1966).
26. H. J. SUE, R. A. PEARSON, D. S. PARKER, J. HUANG and A. F. YEE *Polym. Prepr. Am. Chem. Soc. Div. Polym. Chem.* **29** (1988) 147.
27. S. KUNZ-DOUGLASS, P. W. R. BEAUMONT and M. F. ASHBY, *J. Mater. Sci.* **15** (1980) 1109.
28. S. C. KUNZ and P. W. R. BEAUMONT *ibid.* **16** (1981) 3141.
29. Z. B. AHMAD, M. F. ASHBY and P. W. R. BEAUMONT, *Scrip. Metall.* **20** (1986) 843–848.
30. S. P. WILKINSON, T. C. WARD and J. E. McGRATH, *Polymer* **34** (1993) 870.
31. R. A. PEARSON, Doctoral thesis, University of Michigan, 1990.
32. M. A. PRZYSTUPA and T. H. COURTNEY, *Metall. Trans. A* **13** (1982) 881.
33. A. G. EVANS and R. M. McMEEKING, *Acta Metall.* **34** (1986) 2435.
34. L. S. SIGL, P. A. MATAGA, B. J. DALGLEISH, R. M. McMEEKING and A. G. EVANS, *ibid.* **36** (1988) 945.
35. B. BUDIANSKY, J. C. AMAZIGO and A. G. EVANS, *J. Mech. Phys. Solids* **36** (1988) 167.
36. M. F. ASHBY, F. J. BLUNT and M. BANNISTER, *Acta Metall.* **37** (1989) 1847.
37. H. C. CAO, B. J. DALGLEISH, H. E. DEVE, C. ELLIOTT, A. G. EVANS, R. MEHRABIAN and G. R. ODETTE, *ibid.* **37** (1989) 2969.
38. B. N. COX, *Acta Metall. Mater.* **39** (1991) 1189.
39. M. BANNISTER and M. F. ASHBY, *Acta Metall.* **39** (1991) 2575.
40. M. BANNISTER, H. SHERCLIFF, G. BAO, F. ZOK and M. F. ASHBY, *ibid.* 40 (1992) 1531.
41. G. BAO and F. ZOK, *Acta Metall. Mater.* **41** (1993) 3515.
42. B. N. COX and D. B. MARSHALL, *ibid.* **42** (1994) 341.
43. P. C. PARIS and G. S. SIH, *ASTM STP 381* (1965) 30.
44. F. F. LANGE, *Phil. Mag.* **22** (1970) 983.
45. A. G. EVANS, *ibid.* **26** (1972) 1327.
46. A. J. KINLOCH, D. L. MAXWELL and R. J. YOUNG, *J. Matr. Sci.* **20** (1985) 4169.
47. J. LEE and A. F. YEE, *Polym. Prepr. Am. Chem. Soc. Div. Polym. Chem.* **38** (1997) 369.
48. B. J. CARDWELL, Doctoral thesis, University of Michigan, 1994.
49. J. DU, M. D. THOULESS and A. F. YEE, Development of a process zone in rubber-modified epoxy polymers, *Int. J. Fracture*, accepted.

Received 1 November 1993
and accepted 14 September 1998